CRYSTAL GROWTH & DESIGN

pubs.acs.org/crystal

Article

On the Application of Strong Magnetic Fields during Organic Crystal Growth

Jason Potticary, Charlie L. Hall, Rui Guo, Sarah L. Price, and Simon R. Hall*

Cite This: *Cryst. Growth Des.* 2021, 21, 6254–6265

Read Online

ACCESS | Metrics & More | Article Recommendations | Supporting Information

ABSTRACT: We investigate the effect of crystal growth within a magnetic field for three polymorphic pharmaceuticals, using an experiment where the magnetic field can be varied in strength without altering other crystallization conditions. In the case of carbamazepine, fields above 0.6 T produce metastable form I, and for flufenamic acid, there is an increased propensity to crystallize metastable form I around 1 T. In contrast, the magnetic field has no effect on the crystallization of mefenamic acid, a closely related molecule. The growth of the metastable β polymorph of coronene within a magnetic field at ambient temperature is difficult to reproduce but has been seen as a minor component, consistent with this transformation to the more stable form being facile, depending on the particle size. Calculations of the diamagnetic susceptibility tensors of the polymorphs and their morphologies provide semiquantitative estimates of how the diamagnetic susceptibilities of crystallites differ between polymorphs and explain why mefenamic acid crystallization is unaffected. As the onset of crystallization of carbamazepine and coronene, as defined by changes in turbidity, occur at lower temperatures and hence greater supersaturations in certain ranges of magnetic field strength, this suggests that the field causes precipitation of the metastable form through Ostwald's rule of stages.

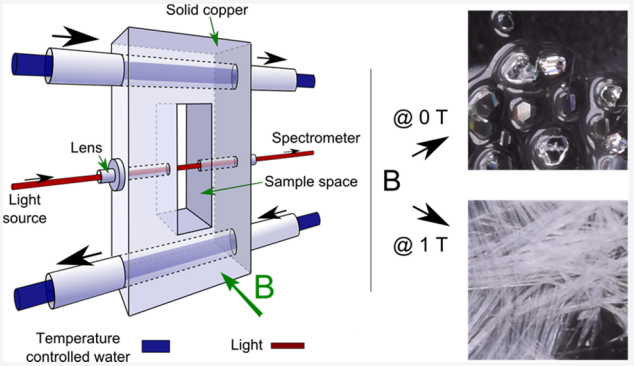

INTRODUCTION

The relationship between the specific crystal structure (polymorph),[1,2] its physical properties, suitable crystallization processes, and the performance of the final product is fundamental[3] to the development and manufacture of pharmaceuticals, food stuffs, dyes, explosives, and functional organic materials such as organic semiconductors.[4] Industry tries to find all polymorphs and hydrates of a specialty chemical, and a range of automated and manual methods have been developed,[5] but this approach often has to be tailored to individual molecules.[6,7] The polymorph screening cannot be restricted to crystallization conditions suitable for manufacture, as the sudden appearance of a more stable form can lead to the loss of control of crystallization of a previously apparently stable form (disappearing polymorphs),[8] and once seeds of a novel polymorph are available, other methods of crystallization may be found. Hence, computational crystal structure prediction (CSP)[9,10] is being developed as a complementary tool[11,12] to polymorph discovery to determine the expected range of polymorphs and their properties.[13] Once the polymorphs have been discovered, then the crystallization of pure phases may require adapting the relative rates of nucleation and growth of the polymorphs, through careful exploration of the variables of the solution, sublimation,[14] or ball-milling[15] crystallization process. Many factors can vary the polymorph produced in a crystallization experiment,[16,17] from pressure,[18] additives,[19] surface templating,[20,21] nanoconfinement[22] to laser-induced nucleation,[23] and so be appropriate methods for polymorph discovery or control.

A less established method of affecting which polymorph is formed could be the application of a magnetic field during crystal growth.[24,25] The effects of a magnetic field on a crystallizing system is a topic that has been sporadically explored over the past few decades mainly on inorganic salts and proteins.[26−30] The influence that an applied field has on such dynamic systems is unknown with numerous, often contradictory, hypotheses and remains to this day, largely, a scientific curio.[31−33] That being said, there are significant potential economic benefits in applications such as removing the need for chemical descalers in the treatment of water to avoid build-up of $CaCO_3$.[34] Recently, we found that a magnetic field had an unexpected effect on the crystallization behavior of the polyaromatic hydrocarbon coronene[35] (Figure 1). Under 1 T of the applied magnetic field, a second

Received: June 22, 2021
Revised: August 24, 2021
Published: September 9, 2021

https://doi.org/10.1021/acs.cgd.1c00723
Cryst. Growth Des. 2021, 21, 6254–6265

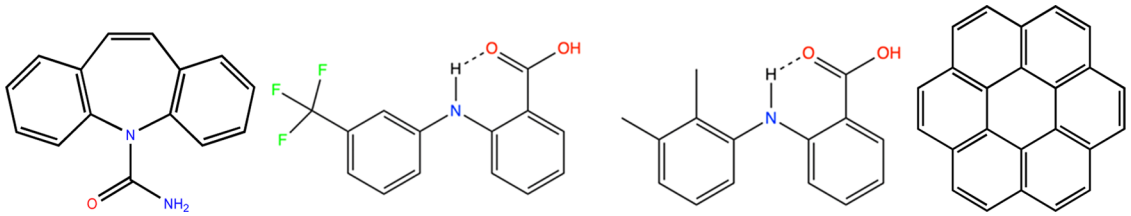

Figure 1. Molecular structures of carbamazepine (CBZ), flufenamic acid (FFA), mefenamic acid (MFA), and coronene.

polymorph (β form) was found to grow under ambient conditions. After an investigation into the thermodynamic stability, it was established that the γ form spontaneously transforms into the β form at low temperatures via an enantiotropic transition.[36−38]

The reports of a magnetic field influencing the crystallization of three distinct organic molecules (2,2′:6′,2″-terpyridine,[24] isoxazolone dye,[25] and coronene[35]) are intriguing. The effect of a magnetic field on a closed-shell molecule is to induce a magnetic moment that opposes the applied field with the relationship between the induced moment and the field direction being described by the diamagnetic susceptibility tensor, χ. For molecules of low symmetry such as organics, the induced moment is at an angle to the applied field as χ depends on the orientation of the conjugated functional groups[39] and so may vary with conformation. The induced moment in a cluster of molecules is a tensorial addition of individual molecular diamagnetic susceptibility tensors and so is dependent on the size and shape of the cluster. The induced magnetic moments in an organic molecule are so small that the thermodynamic effects of a magnetic field are negligible. Even for a molecule with as large an anisotropic diamagnetic susceptibility as coronene, there is only an energy difference of 10^{-3} J mol^{-1} between alignment perpendicular and along a magnetic field of 1 T, which is so much smaller than k_BT at 298 K that the field cannot be affecting the orientational distribution of single molecules in solution. It is not until a molecular cluster of the order of 10^7 coronene molecules is reached that a 1 T magnetic field could produce an energy difference of k_BT at 298 K for different orientations of the molecules. The diamagnetic susceptibility of an organic crystallite is determined by the crystal packing, size, and morphology. From the diamagnetic susceptibility per molecule of the polymorph, the diamagnetic susceptibility of a crystallite of a given size and morphology can be calculated by tensorial addition. A magnetic field has been used to orientate crystallites of diamagnetic organic molecules, to aid determination of the structure by powder X-ray diffraction (PXRD),[40] but by this particle size, a magnetic field is unlikely to produce a major internal rearrangement of the molecules within the crystal.

The implication is that the magnetic field is affecting the kinetics of either nucleation or growth or both. It has been previously reported that higher supersaturations of coronene solutions were attainable under an applied magnetic field, detectable through undercooling of the system.[35] It is also emerging that deviations from classical nucleation theory are observed for many organic molecules, with liquidlike/disordered/densified clusters (without polymorph identity but of a size that would be influenced by a magnetic field) being observed even in undersaturated solutions.[41−43] Thus, there is the potential for a magnetic field to be influencing behavior within prenucleation clusters.

In this work, we determine the effect of strong magnetic fields on the crystallization of three molecular systems that are more typical of pharmaceuticals, namely, carbamazepine, flufenamic acid, and the closely related mefenamic acid (Figure 1). These results, and more insights into the effect of the magnetic field on the crystallization of coronene, are illuminated by the differences in relative stability and magnetic susceptibility tensors of competing polymorphs. Experiments on the effects of the field on the crystallization temperature inform the discussion as to the predictability of whether a magnetic field is able to modify the crystallization of organic molecules.

METHODS

Magnetic Field Crystallization Experiments. A saturated solution of each system was prepared by dissolving the solute in a solvent specific to that molecule (details in the SI, Section I.A). Solute was added to a solvent which was then held at an elevated temperature. Once an equilibrium had been reached between the dissolved and undissolved solute, 3 mL of the solution was extruded through a 0.22 μm PTFE filter to remove any potential nucleation centers or undissolved seeds[44] into a quartz cuvette. For CBZ, FFA, and MFA, the cuvette was then placed inside a copper block preheated to 70 °C, situated between magnetic poles (Figure S1) and left to equilibrate for 1 h. After equilibration, the horizontal linear magnetic field was applied, and the temperature was lowered from 70 to −10 °C at a rate of 1 °C min^{-1}. For coronene, the cuvette was placed in a sample holder (Figure S4) preheated to 90 °C and lowered into the sample space of the Bitter magnet (High Field Magnet Laboratory (HFML), cell 3). A vertical linear magnetic field was applied and, after an equilibration time of 30 min, the temperature was lowered at a rate of 1 °C min^{-1}. Initially, the polymorphic form was established by comparison of the PXRD pattern with those of the known forms. After which, the morphology was used as an identifier, with PXRD used as an occasional control.

Calculation of Diamagnetic Susceptibility Tensors and Lattice Energies. All crystal structures in this paper were first optimized with CASTEP[45] using the PBE functional[46] and Tkatchenko and Scheffler's (TS) dispersion correction scheme,[47] a methodology that is widely used for modeling crystal structures of pharmaceutical molecules,[48,49] particularly in CSP studies.[10] On-the-fly ultrasoft pseudopotentials were used and plane wave cut-off energies and k-point grids were carefully selected for the polymorphs of each molecule to ensure convergence of the total energy (SI Section II). The optimized structures were converged to a maximum force of less than 0.001 eV/Å. The relative energies for these structures were recalculated using the MBD* dispersion correction,[50] to establish the sensitivity of the relative lattice energies to the dispersion model.

The crystal diamagnetic susceptibilities χ^{cryst} of polymorphs were calculated using this charge distribution, using a sum-over-states perturbation expansion for the susceptibility for a magnetic field with finite wavevector, with the macroscopic χ^{cryst} being the limit for a field of infinite wavelength (i.e., uniform B),[51] as previously described.[39] The calculated magnetic susceptibility tensors were diagonalized to find the three eigenvalues, χ_i^{cryst}. From these, the isotropic term, $\chi_{iso}^{cryst} = (\Sigma\chi_i^{cryst})/3$, and anisotropy (the difference between the largest and

https://doi.org/10.1021/acs.cgd.1c00723
Cryst. Growth Des. 2021, 21, 6254−6265

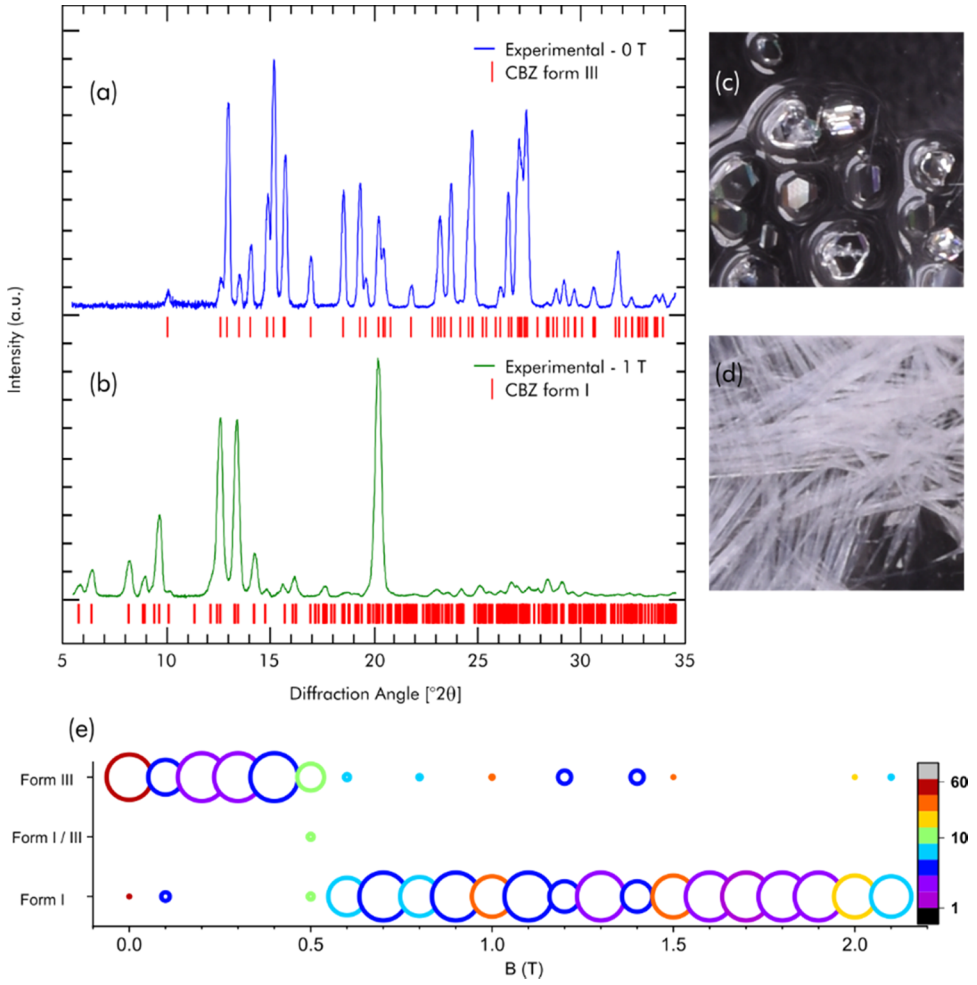

Figure 2. Changes in the polymorph of carbamazepine crystallized from ethanol in varying magnetic fields. Characteristic experimental powder diffraction patterns of (a) form III grown under no field and (b) form I grown at B = 1 T. Optical images of the characteristic morphology of (c) form III and (d) form I. (e) Results of the multiple repeats of the crystallization experiments at each magnetic field strength, color coded by the number of experiments, with the size of the circles representing the relative proportion of the experiments which resulted in the form or mixture specified in the vertical axis.

smallest eigenvalue), $\Delta\chi_{an}^{cryst}$, were calculated. The diamagnetic susceptibility tensor (per molecule within the crystal structure) was overlaid to show its orientation relative to the crystal packing and the main crystal faces, estimated from the crystal structure by the BFDH morphology model[52] calculated using Mercury.[53]

Effect of Magnetic Field on Temperature of Crystallization. In an attempt to quantify the extent to which higher supersaturations were attainable under an applied magnetic field,[35] the temperature of crystallization (C_T) was determined spectroscopically (SI, Section I.B). The samples were prepared as for the crystallization experiments. Once in position, the sample was observed spectroscopically using a deuterium-halogen lamp and monitored using an Ocean Insight Flame USB spectrometer, with C_T being defined at the maximum of the first derivative of the transmission, as a function of temperature (Figure S3). The C_T of coronene in toluene was observed under a range of magnetic fields from 0 to 20 T, in a similar setup in HFML cell 3 (Figure S4), starting at 90 °C at a cooling rate of 1.25 °C min^{-1}. To investigate the parameter space where the effect was maximal, further experiments with a toluene−hexane mixed solvent using the same experimental parameters were carried out at 0.7, 0.8, 0.9, 1.0, 1.1, and 1.2 T in the apparatus shown in Figure S1. Similarly, CBZ was crystallized from ethanol under a range of applied magnetic fields. For flufenamic acid, undercooling experiments were attempted, but extremely high concentrations required resulted in erratic C_T values, and no reliable results were obtained.

RESULTS

Carbamazepine. Carbamazepine (CBZ) (5*H*-dibenz[*b*,*f*]-azepine-5-carboxamide) (Figure 1), an antiepilepsy and trigeminal neuralgia drug, is a well-established polymorphic system and has five known experimental anhydrous forms and a plethora of solvates, though form IV[54] and form V[55] are yet to be produced in solution screening. CBZ has been shown to manifest as either form II or III based on the supersaturation and temperature of the solution from which it was grown.[56]

CBZ III ($P21/c$) has been reported to be the most thermodynamically stable form at atmospheric pressure between 12 K and room temperature.[57,58] Form I ($P\bar{1}$, Z' = 4) is highly metastable and has a close structural relationship[59] with the void-channel-containing CBZ II, whose growth is stabilized by solvent inclusion.[60] When crystallized from ethanol at room temperature, form III is grown from a less saturated solution and form II from a more saturated solution.[56] A region of concomitant growth is also observed as the concentration increases from one region to the other.[56] The pharmaceutically used form III is routinely obtained via evaporation or cooling of an anhydrous ethanol solution. Form I can be accessed from a melt and CBZ III and I are enantiotropically related with a transition temperature at 78

https://doi.org/10.1021/acs.cgd.1c00723
Cryst. Growth Des. 2021, 21, 6254−6265

°C,[61] so form III is the thermodynamically stable of these forms during our crystallization experiments.

When saturated solutions of CBZ in ethanol were cooled in a magnetic field between 0 and 0.4 T, the expected form III is routinely found (95% over approx. 65 experiments). When a magnetic field of >0.5 T is applied, form I is by far the most commonly observed polymorph (88% over approx. 120 experiments) (Figure 2).

Analysis of the diffraction data of the samples crystallized under different fields shows no sign of concomitant polymorphism when the field is under 0.4 T (with most experiments returning pure form III) or over 0.6 T (with most experiments returning pure form I). However, when CBZ crystallizes under an applied field of 0.5 T, some samples were a mixture of forms I and III, though some experiments did give phase-pure form I or phase-pure form III. Furthermore, there is a very strong tendency for a magnetic field above 0.6 T to produce the metastable form I, which rarely occurs at low magnetic fields, with an intermediate field strength sometimes producing a mixed phase.

The only polymorph, other than the expected form III, that was observed in the experiments was form I, which is metastable at ambient temperature. The structure is very different from that in form III, as although both CBZ I and III are based on CBZ hydrogen-bonded dimers, the packing of the aromatic rings is significantly different, giving rise to differences in the anisotropy of the diamagnetic susceptibility tensors (Figure 3). The CBZ I packing is based on "translation stacks" of molecules, while CBZ III is based on so-called "inversion cups", formed by two CBZ molecules.[59] The morphology of crystals is also very different (Figure 2c,d), so although the anisotropy of diamagnetic susceptibility per molecule within the crystals is smaller for form I, the maximum eigenvector has a significant component along the needle axis (Figure 3), and so a sufficiently large crystallite of form I would have a larger diamagnetic anisotropy than form III.

Flufenamic Acid. Flufenamic acid (FFA, *N*-(3-trifluoromethylphenyl)anthranilic acid) (Figure 1) is a fluorinated member of the fenamate group of nonsteroidal anti-inflammatory drugs. It is known to be highly polymorphic,[62] with a number of polymorphs being crystallized at room temperature and pressure in the presence of polymer additives. At room temperature, the two most stable polymorphs, form I and form III, are close in energy, with form III being the most stable structure below 42 °C and form I above this temperature, up to the melting point of the solid.[63] Both polymorphs are accessible via solvent cooling experiments.[64,65]

When FFA crystals are grown from ethanol, the polymorph produced can be affected by the magnetic field (Figure 4), but the outcome is not as reliable as for CBZ (Figure 2). Under zero-field conditions, FFA crystallized as form III, 85.7% of the time with the remaining 14.3% of experiments resulting in form I. As the field is increased to 0.5 T, form I crystallizes more frequently in 66.7% of the experiments, with similar results at 1.0 T. At 2.0 T, however, the appearance of form I becomes less common, reducing to 33.3% of experiments. Although this data is compelling, the extremely high concentration of FFA required for these experiments (600 mg/mL) along with the elevated temperatures, made avoiding any crystallization occurring during solution preparation and transferring extremely challenging, and the FFA experiments

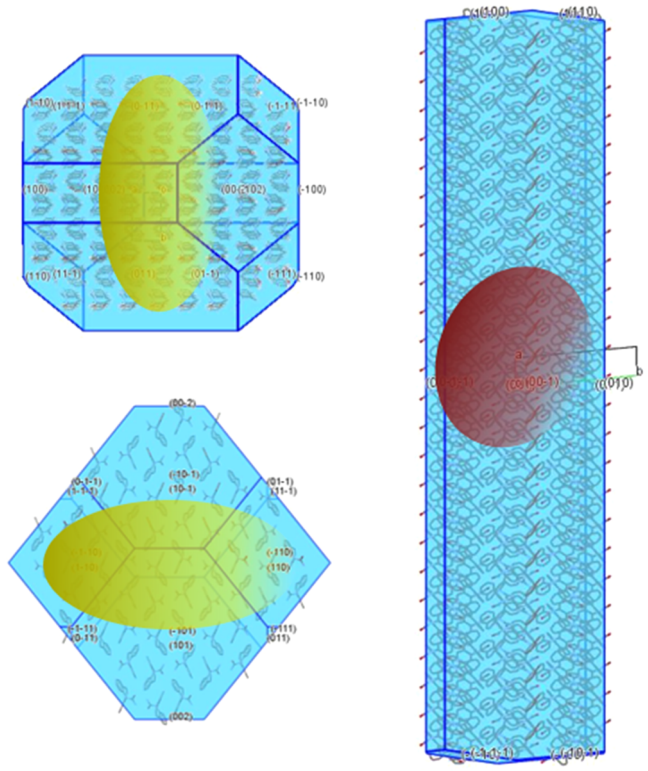

Figure 3. Calculated properties of the observed carbamazepine polymorphs, illustrated by the BFDH morphology of form I and III of CBZ, overlaid with the orientated diamagnetic susceptibility tensor χ ellipsoids, per molecule in the crystal (SI, Table S3). The low symmetry of organic crystals means that the eigenvectors of χ are generally not aligned with the cell axes (SI, Table S3). The properties are calculated with the PBE functional, with the relative lattice energies using the two specified dispersion corrections. Experimental temperature range of stability is taken from ref 60.

are the most likely to be affected by some nucleation occurring prior to switching on the field.

The diamagnetic susceptibility tensor of flufenamic acid is more anisotropic per molecule when in the packing and conformation of form I than form III. There is also a marked difference between the BFDH predicted and observed morphologies (contrast Figures 4 and 5) relative to the difference between the observed morphologies, so it is uncertain how the shape of a growing crystal would determine the anisotropy of the diamagnetic susceptibility of the crystallite. However, FFA molecules adopt very different conformations in the crystals of forms I and III,[39] separated by a sizable energy barrier (i.e., forms I and III are conformational polymorphs[66]), which also contributes to the difference in magnetic susceptibility.

Mefenamic Acid. Mefenamic acid (MFA, 2-[(2,3-dimethylphenyl)amino]benzoic acid) is similar to FFA being

https://doi.org/10.1021/acs.cgd.1c00723
Cryst. Growth Des. 2021, 21, 6254−6265

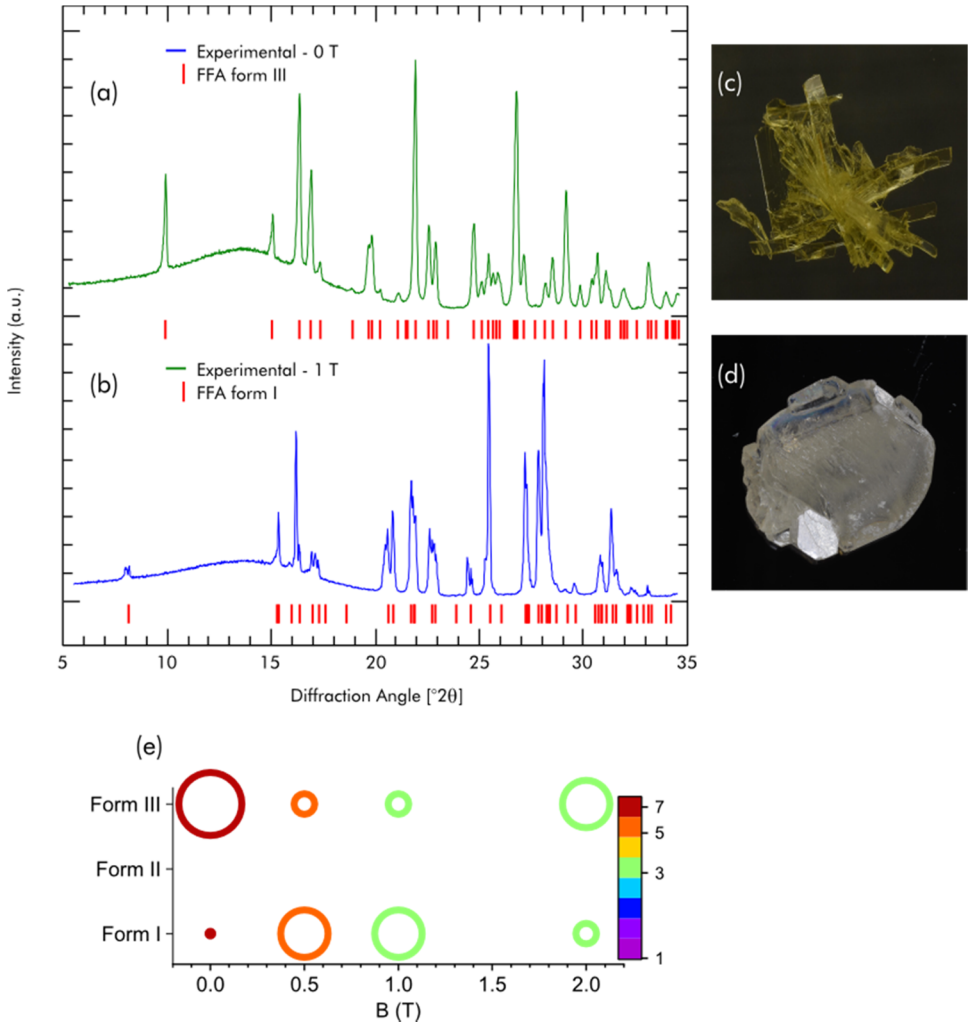

Figure 4. Changes in the polymorph of flufenamic acid crystallized from ethanol in varying magnetic fields. Characteristic powder diffraction patterns of (a) form III, most likely to be grown in field-free conditions, and (b) form I, which usually crystallized at B> 0.5 T. Characteristic morphologies in optical images of (c) form III and (d) form I morphology. (e) Results of the multiple repeats of the crystallization experiments at each magnetic field strength, color coded by the number of experiments, with the size of the circles representing the relative proportion of the experiments which resulted in the form or mixture specified on the vertical axis.

another anthranilic acid derivative, but MFA has only three polymorphs,[67] with form III being highly metastable and found in an attempted cocrystallization experiment with adenine.[67] Form II is stable at elevated temperatures (the transition temperature is 86.6 °C[61]) and form I is the most stable at ambient. Form I crystallizes from most solvents, though form II forms on rapid cooling of DMF solutions, and crystals of form II suitable for structure determination have been prepared by slow evaporation from chloroform in less humid conditions.[67] Form II has also been produced in a high-pressure crystallization experiment.[68] When templated by specific self-assembled monolayers,[69] the nucleation of mefenamic acid from ethanol and methanol shows a preference for form II.[69] Subjected to the same experimental conditions as the previous compounds in this study, MFA showed no polymorph selectivity whatsoever, always crystallizing as form I from ethanol, at any applied magnetic field strength tested (SI, Section I.A.1). The diamagnetic susceptibility tensors for form I and form II (Figure 6) and all other observed crystal structures of mefenamic acid (SI, Section II.A) are very similar. This is because the crystal magnetic susceptibility of a polymorph is largely determined by the relative orientations of the aromatic rings, regardless of whether they are in the same molecule or not, which are similar in all three MFA polymorphs. The MFA conformational polymorphs differ by an approximately 180° change in the torsion angle determining the methyl position, and hence the molecular contribution to χ^{cryst} is similar. Thus, mefenamic acid polymorphs or their nuclei are likely to be affected in similar ways by a magnetic field.

Coronene. The size of a β coronene[a] crystal grown under a magnetic field[35] was sufficient to establish its structure by single-crystal X-ray diffraction. Calculation of the Raman spectra of the two forms has shown that the β form is the more stable phase of coronene at low temperatures,[37,38] which had not previously been characterized because the γ crystals shatter on cooling. Examination of the phase transition in different samples (SI, Section I.D) shows that the polymorphic transformation is dependent on crystal size. As this is a first-order transformation, the degree of hysteresis in the transition is expected to be very dependent on the quality of the crystal, its size, and the cooling rate. The unprecedented growth of a large single crystal of β coronene at ambient in a magnetic field

https://doi.org/10.1021/acs.cgd.1c00723
Cryst. Growth Des. 2021, 21, 6254−6265

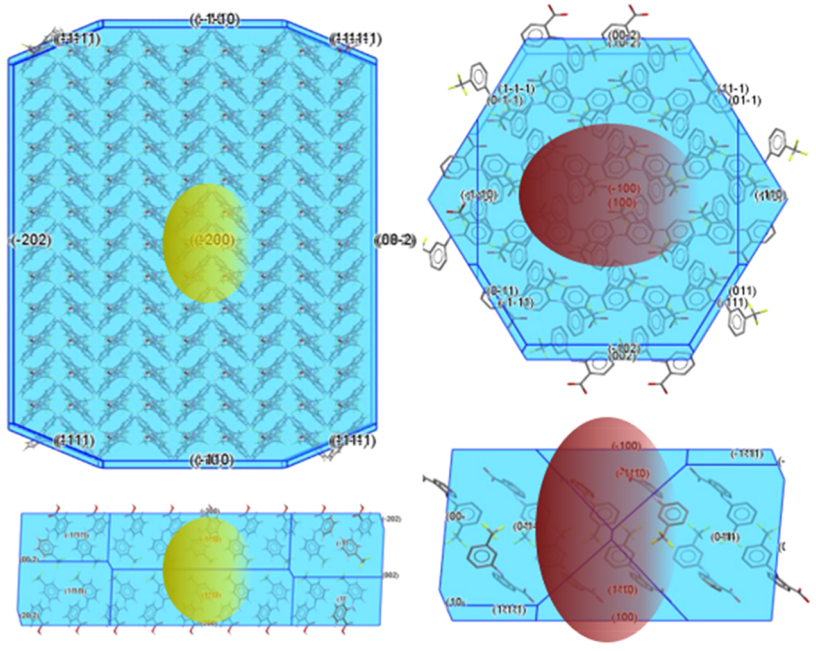

Figure 5. Calculated properties of the observed flufenamic acid polymorphs, illustrated by the BFDH morphology of forms III and I of FFA, overlaid with the orientated diamagnetic susceptibility tensor χ ellipsoids, per molecule in the crystal. The properties are calculated with the PBE functional, with the relative lattice energies including the two specified dispersion corrections. Experimental temperature range of stability taken from ref 62.

gave a crystal that was sufficiently large and perfect that it could be cooled to 80 K for structure determination.

Unfortunately, the reproducibility of the growth of β coronene from the solution at room temperature is difficult; despite repeated attempts for this work, β coronene has only been observed as small crystallites grown concomitantly with γ a small number of times in the alternative apparatus (SI, Figure S4) at the High Field Magnet Laboratory. Periodic DFT-D calculations vary in the relative lattice energies and stability order of the two forms with dispersion correction (Figure 7 with more values in SI, Table S4), but phonon calculations (SI, Section II.C) show that increasing temperature favors the γ form. However, the experimental evidence is clear that β is the low-temperature form, enantiotropically related to the γ form. Crucially, the growth of a single crystal of β in a magnetic field was under conditions when it was metastable. Hence, the inability to reproducibly grow the metastable β polymorph in a magnetic field at ambient temperature seems to be the another case of the phenomenon of "disappearing polymorphs".

Effect of Magnetic Field on Supersaturation/Point of Crystallization. As can be seen from Figure 8, regardless of field strength, the crystallization temperature, C_T, of coronene in toluene is suppressed when compared to zero applied field (C_T = 40 °C). When a linear magnetic field is applied during the cooling of the system, a dramatic change in C_T is observed until a maximum ΔC_T at 0.5 T. This initial, approximately linear suppression of crystallization changes when the field is increased beyond 1.0 T and moves asymptotically toward ΔC_T = 10 °C. This complex behavior suggests that more than one physical attribute of crystallization is being affected by the magnetic field with the most pronounced effect for coronene in toluene occurring between 0.5 and 1.0 T. As the C_T of a saturated solution of coronene in toluene was depressed to 6 °C, a single degree higher than the lowest temperature of which the equipment is capable, a toluene−hexane mixed solvent with a ratio of 1:10 was used to make a saturated solution in which coronene is slightly less soluble, and this was also investigated. The C_T is 21 °C higher in the hexane−toluene mixed solvent than in pure toluene at B = 0 T (Figure 8, left inset and Figure S5). The trend in the mixed solvent system looks similar to that of the toluene-only system, but the largest ΔC_T was considerably smaller (15 °C) than in pure toluene (35 °C), though seen within a similar range of magnetic fields (0.8−1.0 and 0.5−1.0 T).

As with coronene, CBZ was crystallized under a range of applied magnetic fields inside smaller magnets (SI, Figure S1) to look for differences in C_T (Figure 8, right). An increase in applied magnetic field also has a "suppressive" effect on the C_T of CBZ crystals. There is a dramatic change in crystallization temperature with field up to 0.8 T giving a maximum ΔC_T of 59 °C. At higher fields, the suppression of crystallization reduces erratically.

https://doi.org/10.1021/acs.cgd.1c00723
Cryst. Growth Des. 2021, 21, 6254−6265

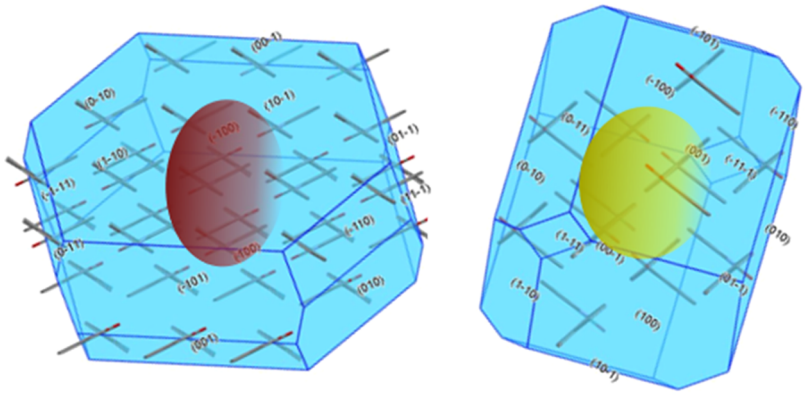

Form I	Form II (major)
Stable below 360 K	Stable above 360 K
ΔE_{latt} (TS) = 0.00 kJ mol^{-1}	ΔE_{latt} (TS) = 2.39 kJ mol^{-1}
ΔE_{latt} (MBD*) = 0.00 kJ mol^{-1}	ΔE_{latt} (MBD*) = 5.10 kJ mol^{-1}
χ_{iso}^{cryst} = -145 cgs-ppm	χ_{iso}^{cryst} = -148 cgs-ppm
$\Delta\chi_{an}^{cryst}$ = -88 cgs-ppm	$\Delta\chi_{an}^{cryst}$ = -70 cgs-ppm
χ_{i}^{cryst} = -105, -137, -193	χ_{i}^{cryst} = -109, -156, -180

Figure 6. Calculated properties of the observed mefenamic acid polymorph, form I, and the alternative polymorph form II, which has been seen in competition with form I in other studies,[69] illustrated by the BFDH morphology, overlaid with the orientated diamagnetic susceptibility tensor χ ellipsoids, per molecule in the crystal. The structure for disordered form II is that of its major component; the results for the minor component of form II and form III are in SI, Table S3. The properties are calculated with the PBE functional, with the relative lattice energies including the two specified dispersion corrections. The experimental temperature range of stability is taken from ref 61.

DISCUSSION

In this work, we investigated the polymorphic outcome in solution cooling crystallizations for four different organic molecules under the influence of an applied magnetic field. CBZ crystallizes in a metastable form in higher applied fields, FFA has a higher rate of crystallizing in a metastable form in fields around 1 T, coronene has been found to crystallize in a metastable form[35] or as a phase impurity (SI, Figure S7) in a field, while the crystallization of MFA is unaffected by the field. All three pharmaceutical molecules have a much smaller average diamagnetic susceptibility per molecule in their polymorphs (χ_{iso}^{mol} between −140 and −150 cgs ppm) compared with coronene (about −265 cgs ppm) as might be expected from the smaller aromatic systems (Figure 1). Nevertheless, for two of the model pharmaceuticals, crystallizing in certain magnetic fields produces a metastable polymorph in experiments that yield the stable form when the field is not switched on. Thus, we have shown that a magnetic field can influence the polymorphic outcome of pharmaceutical molecules. The anisotropy of the diamagnetic susceptibility tensor differs significantly between the polymorphs, except in the case of mefenamic acid, the case where the field does not affect the polymorph observed.

Additional investigations have shown that adjusting the field strength affects the temperature at which a cooling solution crystallizes, showing an "undercooling" effect in coronene and CBZ systems, implying supersaturations greater than those reached when no field is applied. A given concentration is less supersaturated with respect to the metastable form than the stable form, so the undercooling effect would not favor the metastable product. However, Ostwald's rule of stages[70−72] suggests that the metastable form nucleates first, and a greater supersaturation would lead to it crystallizing from solution once the stochastic nucleation process has started, reducing the opportunity for transformation to the more stable form.

If the effect of the magnetic field is merely to suppress nucleation, allowing the metastable form to crystalize, then the nucleation will be stochastic, reflecting the variations in molecular movements. Although our experimental setup has been designed to try to make the experiments only differ in the application of a field, it is perhaps not surprising[73] that it was not possible to reproduce the growth of β coronene under ambient conditions except as a minor phase in a magnetic field or gain reproducible results with flufenamic acid. For coronene, the transition between the two forms is relatively facile, though dependent on sample size (SI, Section I.D). Hence, only crystals of the β form that have grown to a sufficient size and structural purity not to rapidly transform to the stable γ form at ambient could be observed by the time the sample was analyzed by PXRD. In contrast, CBZ does not readily transition between the two forms observed here,[58] which is why we observe the metastable product in abundance. Flufenamic acid, as one of the archetypal polymorphophores,[74] has such a tendency to be trapped in metastable structures[62] that the competition between form I and form III may be influenced by competition with many other polymorphs.

We have no evidence for the magnetic field affecting the polymorphic outcome in a more specific way than altering the relative kinetics of nucleation and growth to favor known metastable forms. Within classical nucleation theory, in which the spherical nucleus has the final structure, its response to a magnetic field will differ between polymorphs, as reflected in the calculated diamagnetic susceptibility anisotropy. However, the polymorph favored by the field is not always the one with

https://doi.org/10.1021/acs.cgd.1c00723
Cryst. Growth Des. 2021, 21, 6254−6265

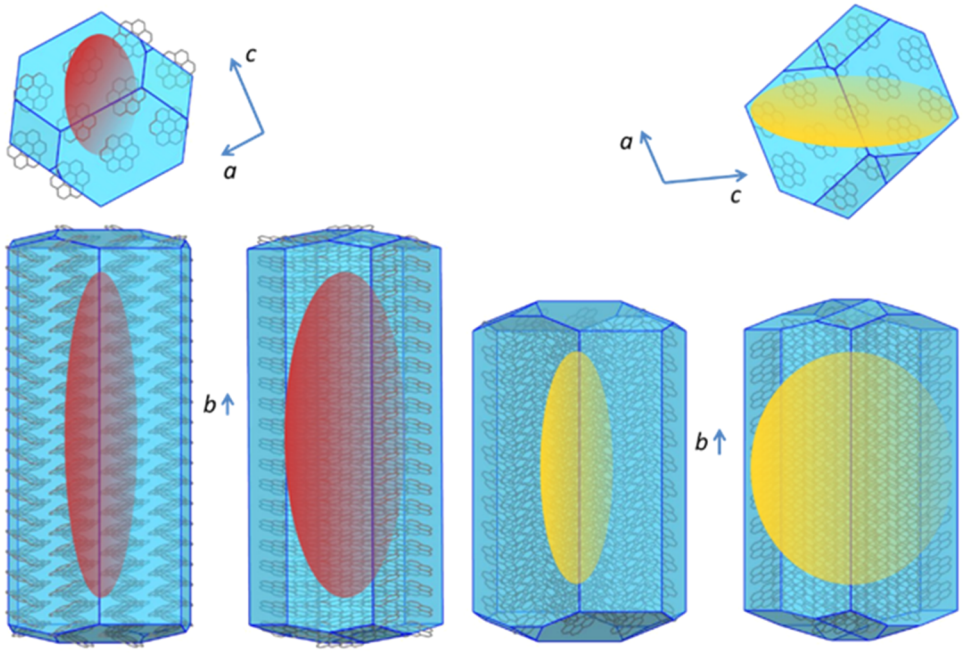

Form β	Form γ
Stable below 160 K	Stable above 160 K
ΔE_{latt} (TS) = 0.00 kJ mol^{-1}	ΔE_{latt} (TS) = 6.79 kJ mol^{-1}
ΔE_{latt} (MBD*) = 0.02 kJ mol^{-1}	ΔE_{latt} (MBD*) = 0.00 kJ mol^{-1}
ΔE_{latt} (D3BJ) = 0.00 kJ mol^{-1}	ΔE_{latt} (D3BJ) = 2.90 kJ mol^{-1}
χ_{iso}^{cryst} = -267 cgs-ppm	χ_{iso}^{cryst} = -262 cgs-ppm
$\Delta\chi_{an}^{cryst}$ = -392 cgs-ppm	$\Delta\chi_{an}^{cryst}$ = -249 cgs-ppm
χ_{i}^{cryst} = -111, -188, -503	χ_{i}^{cryst} = -111, -315, -359

Figure 7. Calculated properties of coronene polymorphs, illustrated by the BFDH morphology overlaid with the orientated diamagnetic susceptibility tensor χ ellipsoids, per molecule in the crystal. The properties are calculated with the PBE functional, with relative lattice energies including the three specified dispersion corrections. The experimental temperature range of stability is from ref 37.

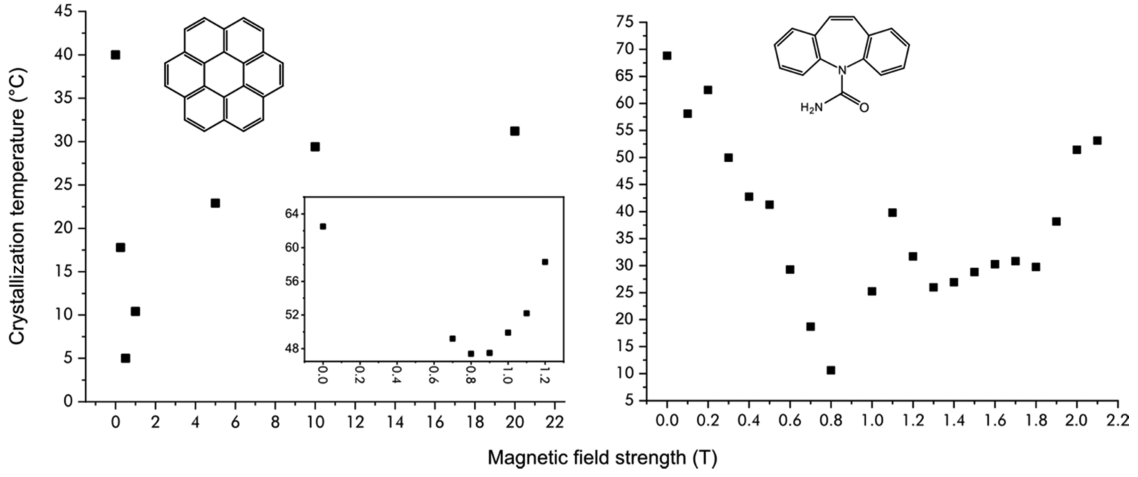

Figure 8. Suppression of crystallization in the (left) coronene−toluene system as a function of magnetic field strength, *B*, up to 20 T. The inset shows a fine variation of *B* around the inflection point conducted using a toluene−hexane mixed solvent from 0 to 1.2 T, to increase the crystallization temperature. (Right) Suppression of crystallization of the CBZ ethanol system as a function of *B*.

the largest magnetic anisotropy. Furthermore, a spherical nanocluster of diameter more than 100 nm with the structure of CBZ III, containing 3×10^6 molecules, would be required before the energy difference between aligning the classical spherical nucleus perpendicular or along a field of 1 T would be comparable to k_BT at ambient temperature. Hence, a

https://doi.org/10.1021/acs.cgd.1c00723
Cryst. Growth Des. 2021, 21, 6254−6265

magnetic field would not be expected to affect the polymorph formed within the classical nucleation theory (CNT). However, we do observe that a magnetic field can affect the crystallization temperature and polymorphic outcome implying that CNT does not correctly describe these systems.

The magnetic susceptibility of a crystallite is affected by its size and shape, as it is tensorially additive, and some of the competing polymorph pairs differ in morphology. Orientated or rotating growing crystallites could modify the approach of solute growth units to the nascent crystallite and possibly affect the growth spirals. Magnetic fields with gradients can suppress the surface convections, thus slowing down the growth of protein crystals,[75,76] though our experiments are in a uniform field. If the field is affecting the structure of the surface layer and local supersaturation, then this can affect the relative thermodynamic stability of the polymorphs at small nuclei/crystallite sizes.[77] Although it is plausible that the field differentially affects crystallite growth, it seems more likely that the field is affecting the formation of prenucleation clusters in which there is an increased density of solute molecules, but the cluster is still liquidlike. In this type of two-step nucleation, there are many factors that can influence which polymorph emerges, such as the presence of surfaces.[78] It is conceivable that the field may make a difference to the organization of the molecules within the dense solvent−solute cluster, but elucidating the mechanism would require more experimental work.[41,42] With a molecular-level model of a nucleating cluster, it would be feasible to estimate its magnetic susceptibility, assuming tensorial addition of the molecular susceptibility, which is a good approximation for crystals.[39]

If the magnetic field always favors metastable polymorphs, then it may be a useful additional tool in polymorph control when a metastable form is needed. There is also the potential of combining crystal structure prediction studies with the estimate of the magnetic susceptibility tensor to produce energy-structure- $\Delta\chi_{an}^{cryst}$ maps[39] to determine whether there are unobserved structures that are energetically competitive with the known forms, whose crystallization could be more favorable in a magnetic field. Such a map is shown in Figure 9 for coronene, where it is clear that the β form is not only close in energy to the γ form that is usually crystallized at ambient but also will be more affected by a magnetic field, suggesting that magnetic field-induced polymorph change is a distinct possibility. The magnetic field could not affect the polymorphic outcome if the diamagnetic susceptibility tensor was the same for each polymorph (as found for mefenamic acid (Figure 6)), so such property crystal energy landscapes can at least show when there are no thermodynamically competitive unseen structures whose nucleation may be affected by a magnetic field.

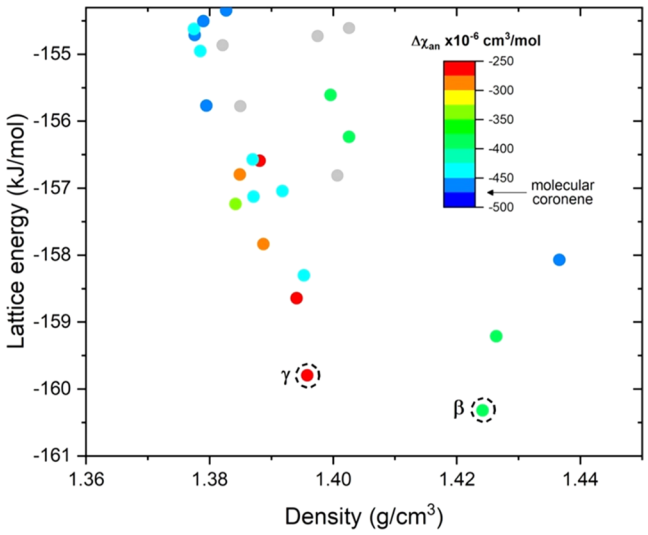

Figure 9. Summary of the output of a CSP study on coronene, where each symbol represents a minimum in the lattice energy, colored by the anisotropy in the diamagnetic susceptibility.

In summary, crystallization in a magnetic field is a technique that may affect polymorphic outcome and so could be considered as a route to finding more polymorphs. This effect needs consideration when an applied field is necessary during analysis (e.g., in most transmission electron microscopes).[79] However, far more needs to be understood about the nucleation of organic molecules before it can be considered as a reliable route to polymorph control for specific pharmaceutical systems.

CONCLUSIONS

We have demonstrated that a magnetic field can affect the polymorphic outcome of crystallization of model pharmaceutical molecules, containing typical aromatic systems, provided that they are packed to give a significant difference in the anisotropy of the diamagnetic susceptibility tensor. For carbamazepine, the crystallization of metastable form I at fields greater than 0.6 T is reasonably reproducible (Figure 2). In the case of flufenamic acid, there is a switch in whether form III or I is preferred over a range of fields. On the basis of this limited range of compounds, it seems that the magnetic field can help stabilize the nucleation of the metastable form. This is likely to occur from the magnetic field suppressing nucleation, leading to a higher supersaturation when crystallization occurs. More work is needed to understand crystallization in a magnetic field, but calculations can establish when a magnetic field could not distinguish between polymorphs as shown for mefenamic acid.

ASSOCIATED CONTENT

Supporting Information

The Supporting Information is available free of charge at https://pubs.acs.org/doi/10.1021/acs.cgd.1c00723.

Referenced data schematic (a) and images (b−d) of the experimental setup for the magnetic crystallization experiments (Figure S1); powder diffraction patterns of crystals of MFA (Figure S2); schematic of interpretation of C_T (Figure S3); experimental setup of in situ crystallization experiments (Figure S4); transmission as a function of temperature (Figure S5); concomitant polycrystalline growth (Figure S6); size-dependent phase transitions in coronene (Figure S7); phonon dispersion of coronene β form (Figure S8); calculated Helmholtz free energy (A), internal energy (U), and TS terms of coronene β and γ form (Figure S9); different contributions to the Helmholtz free energy difference (Figure S10); and detailed experimental information and computational methods (PDF)

https://doi.org/10.1021/acs.cgd.1c00723
Cryst. Growth Des. 2021, 21, 6254−6265

AUTHOR INFORMATION

Corresponding Author

Simon R. Hall − *Complex Functional Materials Group, School of Chemistry, University of Bristol, Bristol BS8 1TS, U.K.;* orcid.org/0000-0002-2816-0191; Email: simon.hall@bristol.ac.uk

Authors

Jason Potticary − *Complex Functional Materials Group, School of Chemistry, University of Bristol, Bristol BS8 1TS, U.K.;* orcid.org/0000-0003-0462-4980

Charlie L. Hall − *Complex Functional Materials Group, School of Chemistry, University of Bristol, Bristol BS8 1TS, U.K.; Centre for Doctoral Training in Condensed Matter Physics, HH Wills Physics Laboratory, Bristol BS8 1TL, U.K.;* orcid.org/0000-0002-4692-6138

Rui Guo − *Department of Chemistry, University College London, London WC1H 0AJ, U.K;* orcid.org/0000-0002-1129-4716

Sarah L. Price − *Department of Chemistry, University College London, London WC1H 0AJ, U.K;* orcid.org/0000-0002-1230-7427

Complete contact information is available at: https://pubs.acs.org/10.1021/acs.cgd.1c00723

Author Contributions

S.R.H. initiated and supervised the project. J.P. and C.H. performed the crystallization and structural characterization experiments at Bristol. R.G. performed the CASTEP calculations under the supervision of S.L.P. at UCL. All authors contributed to the discussion of the results, analysis of the materials, and to manuscript preparation.

Funding

This work is supported by MagnaPharm, a collaborative research project funded by the European Union's Horizon 2020 Research and Innovation programme under Grant Agreement Number 736899. S.R.H., J.P., and C.H. acknowledge the Engineering and Physical Sciences Research Council UK (grants EP/L015544/1) and the Bristol Centre for Functional Nanomaterials and the Centre for Doctoral Training in Condensed Matter Physics for project funding. Part of the computational work was carried out on ARCHER, UK National Supercomputing Service (http://www.archer.ac.uk) via our membership of the UK's HEC Materials Chemistry Consortium, which is funded by EPSRC (EP/L000202).

Notes

The authors declare no competing financial interest.

ACKNOWLEDGMENTS

R.G. acknowledges the help of Prof. Jonathan Yates, Dr. Simone Sturniolo, and CCP-NC, Collaborative Computational Project for NMR crystallography, for carrying out magnetic property calculations with CASTEP. The authors would like to thank Emily Luke for her help with the supplementary cover art.

ADDITIONAL NOTE

[a]Please note that the correct nomenclature of beta- and gamma-coronene uses non-italicized Greek characters (see reference 35). The font used in this manuscript gives them the appearance that they are in italics, but they are not.

REFERENCES

(1) Bernstein, J. *Polymorphism in Molecular Crystals*; Clarendon Press: Oxford, 2020.

(2) Hilfiker, R.; von Raumer, M. *Polymorphism in the Pharmaceutical Industry, Solid Form and Drug Development*, 2nd ed.; Wiley-VCH: Weinheim, Germany, 2019.

(3) Sun, C. C. Materials Science Tetrahedron—A Useful Tool for Pharmaceutical Research and Development. *J. Pharm. Sci.* **2009**, *98*, 1671−1687.

(4) Yang, Y.; Rice, B.; Shi, X.; Brandt, J. R.; Correa da Costa, R.; Hedley, G. J.; Smilgies, D.-M.; Frost, J. M.; Samuel, I. D. W.; Otero-de-la-Roza, A.; Johnson, E. R.; Jelfs, K. E.; Nelson, J.; Campbell, A. J.; Fuchter, M. J. Emergent Properties of an Organic Semiconductor Driven by Its Molecular Chirality. *ACS Nano* **2017**, *11*, 8329−8338.

(5) Pfund, L. Y.; Matzger, A. J. Towards Exhaustive and Automated High-Throughput Screening for Crystalline Polymorphs. *ACS Comb. Sci.* **2014**, *16*, 309−313.

(6) Newman, A. Specialized Solid Form Screening Techniques. *Org. Process Res. Dev.* **2013**, *17*, 457−471.

(7) Bhardwaj, R. M.; McMahon, J. A.; Nyman, J.; Price, L. S.; Konar, S.; Oswald, I. D. H.; Pulham, C. R.; Price, S. L.; Reutzel-Edens, S. M. A Prolific Solvate Former, Galunisertib, under the Pressure of Crystal Structure Prediction, Produces Ten Diverse Polymorphs. *J. Am. Chem. Soc.* **2019**, *141*, 13887−13897.

(8) Bučar, D.-K.; Lancaster, R. W.; Bernstein, J. Disappearing Polymorphs Revisited. *Angew. Chem., Int. Ed.* **2015**, *54*, 6972−6993.

(9) Reilly, A. M.; Cooper, R. I.; Adjiman, C. S.; Bhattacharya, S.; Boese, A. D.; Brandenburg, J. G.; Bygrave, P. J.; Bylsma, R.; Campbell, J. E.; Car, R.; Case, D. H.; Chadha, R.; Cole, J. C.; Cosburn, K.; Cuppen, H. M.; Curtis, F.; Day, G. M.; DiStasio, R. A., Jr; Dzyabchenko, A.; van Eijck, B. P.; Elking, D. M.; van den Ende, J. A.; Facelli, J. C.; Ferraro, M. B.; Fusti-Molnar, L.; Gatsiou, C.-A.; Gee, T. S.; de Gelder, R.; Ghiringhelli, L. M.; Goto, H.; Grimme, S.; Guo, R.; Hofmann, D. W. M.; Hoja, J.; Hylton, R. K.; Iuzzolino, L.; Jankiewicz, W.; de Jong, D. T.; Kendrick, J.; de Klerk, N. J. J.; Ko, H.-Y.; Kuleshova, L. N.; Li, X.; Lohani, S.; Leusen, F. J. J.; Lund, A. M.; Lv, J.; Ma, Y.; Marom, N.; Masunov, A. E.; McCabe, P.; McMahon, D. P.; Meekes, H.; Metz, M. P.; Misquitta, A. J.; Mohamed, S.; Monserrat, B.; Needs, R. J.; Neumann, M. A.; Nyman, J.; Obata, S.; Oberhofer, H.; Oganov, A. R.; Orendt, A. M.; Pagola, G. I.; Pantelides, C. C.; Pickard, C. J.; Podeszwa, R.; Price, L. S.; Price, S. L.; Pulido, A.; Read, M. G.; Reuter, K.; Schneider, E.; Schober, C.; Shields, G. P.; Singh, P.; Sugden, I. J.; Szalewicz, K.; Taylor, C. R.; Tkatchenko, A.; Tuckerman, M. E.; Vacarro, F.; Vasileiadis, M.; Vazquez-Mayagoitia, A.; Vogt, L.; Wang, Y.; Watson, R. E.; de Wijs, G. A.; Yang, J.; Zhu, Q.; Groom, C. R. Report on the Sixth Blind Test of Organic Crystal Structure Prediction Methods. *Acta Crystallogr., Sect. B: Struct. Sci., Cryst. Eng. Mater.* **2016**, *72*, 439−459.

(10) Price, S. L. Is Zeroth Order Crystal Structure Prediction (CSP_0) Coming to Maturity? What Should We Aim for in an Ideal Crystal Structure Prediction Code? *Faraday Discuss.* **2018**, *211*, 9−30.

(11) Price, S. L.; Reutzel-Edens, S. M. The Potential of Computed Crystal Energy Landscapes to Aid Solid-Form Development. *Drug Discovery Today* **2016**, *21*, 912−923.

(12) Nyman, J.; Reutzel-Edens, S. M. Crystal Structure Prediction Is Changing from Basic Science to Applied Technology. *Faraday Discuss.* **2018**, *211*, 459−476.

(13) Musil, F.; De, S.; Yang, J.; Campbell, J. E.; Day, G. M.; Ceriotti, M. Machine Learning for the Structure−Energy−Property Landscapes of Molecular Crystals. *Chem. Sci.* **2018**, *9*, 1289−1300.

(14) Kamali, N.; O'Malley, C.; Mahon, M. F.; Erxleben, A.; McArdle, P. Use of Sublimation Catalysis and Polycrystalline Powder Templates for Polymorph Control of Gas Phase Crystallization. *Cryst. Growth Des.* **2018**, *18*, 3510−3516.

(15) Kamali, N.; Gniado, K.; McArdle, P.; Erxleben, A. Application of Ball Milling for Highly Selective Mechanochemical Polymorph Transformations. *Org. Process Res. Dev.* **2018**, *22*, 796−802.

(16) Llinàs, A.; Goodman, J. M. Polymorph Control: Past, Present and Future. *Drug Discovery Today* **2008**, *13*, 198−210.

(17) Lee, E. H. A Practical Guide to Pharmaceutical Polymorph Screening & Selection. Asian. *J. Pharm. Sci.* **2014**, *9*, 163−175.
(18) Fabbiani, F. P. A.; Pulham, C. R. High-Pressure Studies of Pharmaceutical Compounds and Energetic Materials. *Chem. Soc. Rev.* **2006**, *35*, 932.
(19) Bučar, D.-K.; Day, G. M.; Halasz, I.; Zhang, G. G. Z.; Sander, J. R. G.; Reid, D. G.; MacGillivray, L. R.; Duer, M. J.; Jones, W. The Curious Case of (Caffeine)·(Benzoic Acid): How Heteronuclear Seeding Allowed the Formation of an Elusive Cocrystal. *Chem. Sci.* **2013**, *4*, 4417.
(20) Solomos, M. A.; Capacci-Daniel, C.; Rubinson, J. F.; Swift, J. A. Polymorph Selection via Sublimation onto Siloxane Templates. *Cryst. Growth Des.* **2018**, *18*, 6965−6972.
(21) Case, D. H.; Srirambhatla, V. K.; Guo, R.; Watson, R. E.; Price, L. S.; Polyzois, H.; Cockcroft, J. K.; Florence, A. J.; Tocher, D. A.; Price, S. L. Successful Computationally Directed Templating of Metastable Pharmaceutical Polymorphs. *Cryst. Growth Des.* **2018**, *18*, 5322−5331.
(22) Ward, M. D. Perils of Polymorphism: Size Matters. *Isr. J. Chem.* **2017**, *57*, 82−92.
(23) Clair, B.; Ikni, A.; Li, W.; Scouflaire, P.; Quemener, V.; Spasojević-de Biré, A. A New Experimental Setup for High-Throughput Controlled Non-Photochemical Laser-Induced Nucleation: Application to Glycine Crystallization. *J. Appl. Crystallogr.* **2014**, *47*, 1252−1260.
(24) Honjo, S.; Yokota, M.; Doki, N.; Shimizu, K. Magnetic Field Influence on the Crystal Structure of 2,2′:6′,2″-Terpyridine. *Kagaku Kogaku Ronbunshu* **2008**, *34*, 383−387.
(25) Aret, E.; Radboud, R. *Growth of Organic Dye Crystals Morphology and Polymorphism*; Radboud University, 2013; pp 109−119.
(26) Kuschel, F.; König, A.; Gropp, R. Crystal Growth in Magnetic Fields (I) Crystallization of Me (NH4)2(SO4)2 · 6 H2O (Me = Zn, Cu, Ni, Fe) from Aqueous Solutions in Moderate Magnetic Fields. *Cryst. Res. Technol.* **1982**, *17*, 793−799.
(27) Freitas, A. M. B.; Landgraf, F. J. G.; Nvltý, J.; Giulietti, M. Influence of Magnetic Field in the Kinetics of Crystallization of Diamagnetic and Paramagnetic Inorganic Salts. *Cryst. Res. Technol.* **1999**, *34*, 1239−1244.
(28) Wakayama, N. I. Effects of a Strong Magnetic Field on Protein Crystal Growth. *Cryst. Growth Des.* **2003**, *3*, 17−24.
(29) Tai, C. Y.; Wu, C. K.; Chang, M. C. Effects of Magnetic Field on the Crystallization of CaCO3 Using Permanent Magnets. *Chem. Eng. Sci.* **2008**, *63*, 5606−5612.
(30) Rodzevich, A. P.; Kuzmina, L. V.; Gazenaur, E. G.; Sugatov, E. V.; Krasheninin, V. I. The Effect of Magnetic Field on Crystallization and Some Properties of Silver Azide Crystals. *Mater. Sci. Forum* **2018**, *938*, 18−26.
(31) Amiri, M. C.; Dadkhah, A. A. On Reduction in the Surface Tension of Water Due to Magnetic Treatment. *Colloids Surf., A* **2006**, *278*, 252−255.
(32) Wang, Y.; Zhang, B.; Gong, Z.; Gao, K.; Ou, Y.; Zhang, J. The Effect of a Static Magnetic Field on the Hydrogen Bonding in Water Using Frictional Experiments. *J. Mol. Struct.* **2013**, *1052*, 102−104.
(33) Cai, R.; Yang, H.; He, J.; Zhu, W. The Effects of Magnetic Fields on Water Molecular Hydrogen Bonds. *J. Mol. Struct.* **2009**, *938*, 15−19.
(34) Lin, L.; Jiang, W.; Xu, X.; Xu, P. A Critical Review of the Application of Electromagnetic Fields for Scaling Control in Water Systems: Mechanisms, Characterization, and Operation. *npj Clean Water* **2020**, *3*, No. 25.
(35) Potticary, J.; Terry, L. R.; Bell, C.; Papanikolopoulos, A. N.; Christianen, P. C. M.; Engelkamp, H.; Collins, A. M.; Fontanesi, C.; Kociok-Köhn, G.; Crampin, S.; Da Como, E.; Hall, S. R. An Unforeseen Polymorph of Coronene by the Application of Magnetic Fields during Crystal Growth. *Nat. Commun.* **2016**, No. 11555.
(36) Potticary, J.; Boston, R.; Vella-Zarb, L.; Few, A.; Bell, C.; Hall, S. R. Low Temperature Magneto-Morphological Characterisation of Coronene and the Resolution of Previously Observed Unexplained Phenomena. *Sci. Rep.* **2016**, *6*, No. 38696.
(37) Bannister, N.; Skelton, J.; Kociok-Köhn, G.; Batten, T.; Da Como, E.; Crampin, S. Lattice Vibrations of γ- and β-Coronene from Raman Microscopy and Theory. *Phys. Rev. Mater.* **2019**, *3*, No. 125601.
(38) Salzillo, T.; Giunchi, A.; Masino, M.; Bedoya-Martínez, N.; Della Valle, R. G.; Brillante, A.; Girlando, A.; Venuti, E. An Alternative Strategy to Polymorph Recognition at Work: The Emblematic Case of Coronene. *Cryst. Growth Des.* **2018**, *18*, 4869−4873.
(39) Guo, R.; Uddin, M. N.; Price, L. S.; Price, S. L. Calculation of Diamagnetic Susceptibility Tensors of Organic Crystals: From Coronene to Pharmaceutical Polymorphs. *J. Phys. Chem. A* **2020**, *124*, 1409−1420.
(40) Kimura, F.; Kimura, T. Magnetically Textured Powders—an Alternative to Single-Crystal and Powder X-Ray Diffraction Methods. *CrystEngComm* **2018**, *20*, 861−872.
(41) Warzecha, M.; Safari, M. S.; Florence, A. J.; Vekilov, P. G. Mesoscopic Solute-Rich Clusters in Olanzapine Solutions. *Cryst. Growth Des.* **2017**, *17*, 6668−6676.
(42) Cookman, J.; Hamilton, V.; Hall, S. R.; Bangert, U. Non-Classical Crystallisation Pathway Directly Observed for a Pharmaceutical Crystal via Liquid Phase Electron Microscopy. *Sci. Rep.* **2020**, *10*, No. 19156.
(43) Cookman, J.; Hamilton, V.; Price, L. S.; Hall, S. R.; Bangert, U. Visualising Early-Stage Liquid Phase Organic Crystal Growth via Liquid Cell Electron Microscopy. *Nanoscale* **2020**, *12*, 4636−4644.
(44) Kuhs, M.; Zeglinski, J.; Rasmuson, Å. C. Influence of History of Solution in Crystal Nucleation of Fenoxycarb: Kinetics and Mechanisms. *Cryst. Growth Des.* **2014**, *14*, 905−915.
(45) Clark, S. J.; Segall, M. D.; Pickard, C. J.; Hasnip, P. J.; Probert, M. I. J.; Refson, K.; Payne, M. C. First Principles Methods Using CASTEP. *Z. Kristallogr. - Cryst. Mater.* **2005**, *220*, 567−570.
(46) Perdew, J. P.; Burke, K.; Ernzerhof, M. Generalized Gradient Approximation Made Simple. *Phys. Rev. Lett.* **1996**, *77*, 3865−3868.
(47) Tkatchenko, A.; Scheffler, M. Accurate Molecular Van Der Waals Interactions from Ground-State Electron Density and Free-Atom Reference Data. *Phys. Rev. Lett.* **2009**, *102*, No. 073005.
(48) van de Streek, J.; Neumann, M. A. Validation of Experimental Molecular Crystal Structures with Dispersion-Corrected Density Functional Theory Calculations. *Acta Crystallogr., Sect. B: Struct. Sci.* **2010**, *66*, 544−558.
(49) Beran, G. J. O. Modeling Polymorphic Molecular Crystals with Electronic Structure Theory. *Chem. Rev.* **2016**, *116*, 5567−5613.
(50) Ambrosetti, A.; Reilly, A. M.; DiStasio, R. A.; Tkatchenko, A. Long-Range Correlation Energy Calculated from Coupled Atomic Response Functions. *J. Chem. Phys.* **2014**, *140*, No. 18A508.
(51) Mauri, F.; Louie, S. G. Magnetic Susceptibility of Insulators from First Principles. *Phys. Rev. Lett.* **1996**, *76*, 4246−4249.
(52) Docherty, R.; Clydesdale, G.; Roberts, K. J.; Bennema, P. Application of Bravais-Friedel-Donnay-Harker, Attachment Energy and Ising Models to Predicting and Understanding the Morphology of Molecular Crystals. *J. Phys. D. Appl. Phys.* **1991**, *24*, 89−99.
(53) Macrae, C. F.; Sovago, I.; Cottrell, S. J.; Galek, P. T. A.; McCabe, P.; Pidcock, E.; Platings, M.; Shields, G. P.; Stevens, J. S.; Towler, M.; Wood, P. A. Mercury 4.0: From Visualization to Analysis, Design and Prediction. *J. Appl. Crystallogr.* **2020**, *53*, 226−235.
(54) Florence, A. J.; Johnston, A.; Price, S. L.; Nowell, H.; Kennedy, A. R.; Shankland, N. An Automated Parallel Crystallisation Search for Predicted Crystal Structures and Packing Motifs of Carbamazepine. *J. Pharm. Sci.* **2006**, *95*, 1918−1930.
(55) Arlin, J.-B.; Price, L. S.; Price, S. L.; Florence, A. J. A Strategy for Producing Predicted Polymorphs: Catemeric Carbamazepine Form V. *Chem. Commun.* **2011**, *47*, 7074.
(56) Parambil, J. V.; Poornachary, S. K.; Tan, R. B. H.; Heng, J. Y. Y. Influence of Solvent Polarity and Supersaturation on Template-Induced Nucleation of Carbamazepine Crystal Polymorphs. *J. Cryst. Growth* **2017**, *469*, 84−90.

https://doi.org/10.1021/acs.cgd.1c00723
Cryst. Growth Des. 2021, 21, 6254−6265

(57) Grzesiak, A. L.; Lang, M.; Kim, K.; Matzger, A. J. Comparison of the Four Anhydrous Polymorphs of Carbamazepine and the Crystal Structure of Form I. *J. Pharm. Sci.* **2003**, *92*, 2260−2271.
(58) Brandenburg, J. G.; Potticary, J.; Sparkes, H. A.; Price, S. L.; Hall, S. R. Thermal Expansion of Carbamazepine: Systematic Crystallographic Measurements Challenge Quantum Chemical Calculations. *J. Phys. Chem. Lett.* **2017**, *8*, 4319−4324.
(59) Gelbrich, T.; Hursthouse, M. B. Systematic Investigation of the Relationships between 25 Crystal Structures Containing the Carbamazepine Molecule or a Close Analogue: A Case Study of the XPac Method. *CrystEngComm* **2006**, *8*, 448.
(60) Cruz Cabeza, A. J.; Day, G. M.; Motherwell, W. D. S.; Jones, W. Solvent Inclusion in Form II Carbamazepine. *Chem. Commun.* **2007**, *16*, 1600.
(61) Park, K.; Evans, J. M. B.; Myerson, A. S. Determination of Solubility of Polymorphs Using Differential Scanning Calorimetry. *Cryst. Growth Des.* **2003**, *3*, 991−995.
(62) López-Mejías, V.; Kampf, J. W.; Matzger, A. J. Nonamorphism in Flufenamic Acid and a New Record for a Polymorphic Compound with Solved Structures. *J. Am. Chem. Soc.* **2012**, *134*, 9872−9875.
(63) Li, H.; Wen, H.; Stowell, J. G.; Morris, K. R.; Byrn, S. R. Crystal Quality and Physical Reactivity in the Case of Flufenamic Acid (FFA). *J. Pharm. Sci.* **2010**, *99*, 3839−3848.
(64) Delaney, S. P.; Smith, T. M.; Korter, T. M. Conformational Origins of Polymorphism in Two Forms of Flufenamic Acid. *J. Mol. Struct.* **2014**, *1078*, 83−89.
(65) Krishna Murthy, H. M.; Bhat, T. N.; Vijayan, M. Structure of a New Crystal Form of 2-{[3-(Trifluoromethyl)Phenyl]Amino}benzoic Acid (Flufenamic Acid). *Acta Crystallogr., Sect. B: Struct. Crystallogr. Cryst. Chem.* **1982**, *38*, 315−317.
(66) Cruz-Cabeza, A. J.; Bernstein, J. Conformational Polymorphism. *Chem. Rev.* **2014**, *114*, 2170−2191.
(67) SeethaLekshmi, S.; Guru Row, T. N. Conformational Polymorphism in a Non-Steroidal Anti-Inflammatory Drug, Mefenamic Acid. *Cryst. Growth Des.* **2012**, *12*, 4283−4289.
(68) Abbas, N.; Oswald, I.; Pulham, C. Accessing Mefenamic Acid Form II through High-Pressure Recrystallisation. *Pharmaceutics* **2017**, *9*, 16.
(69) Yang, X.; Sarma, B.; Myerson, A. S. Polymorph Control of Micro/Nano-Sized Mefenamic Acid Crystals on Patterned Self-Assembled Monolayer Islands. *Cryst. Growth Des.* **2012**, *12*, 5521−5528.
(70) Cardew, P. T.; Davey, R. J. The Ostwald Ratio, Kinetic Phase Diagrams, and Polymorph Maps. *Cryst. Growth Des.* **2019**, *19*, 5798−5810.
(71) Threlfall, T. Structural and Thermodynamic Explanations of Ostwald's Rule. *Org. Process Res. Dev.* **2003**, *7*, 1017−1027.
(72) Ostwald, W. Studies on the Formation and Transformation of Solid Bodies. *Z. Phys. Chem.* **1897**, *22*, 289−330.
(73) Threlfall, T. Crystallisation of Polymorphs: Thermodynamic Insight into the Role of Solvent. *Org. Process Res. Dev.* **2000**, *4*, 384−390.
(74) López-Mejías, V.; Matzger, A. J. Structure−Polymorphism Study of Fenamates: Toward Developing an Understanding of the Polymorphophore. *Cryst. Growth Des.* **2015**, *15*, 3955−3962.
(75) Heijna, M. C. R.; Poodt, P. W. G.; Tsukamoto, K.; De Grip, W. J.; Christianen, P. C. M.; Maan, J. C.; Hendrix, J. L. A.; Van Enckevort, W. J. P.; Vlieg, E. Magnetically Controlled Gravity for Protein Crystal Growth. *Appl. Phys. Lett.* **2007**, *90*, No. 264105.
(76) Poodt, P. W. G.; Heijna, M. C. R.; Tsukamoto, K.; De Grip, W. J.; Christianen, P. C. M.; Maan, J. C.; Van Enckevort, W. J. P.; Vlieg, E. Suppression of Convection Using Gradient Magnetic Fields during Crystal Growth of $NiSO_4 \cdot 6H_2O$. *Appl. Phys. Lett.* **2005**, *87*, 1−3.
(77) Belenguer, A. M.; Lampronti, G. I.; Cruz-Cabeza, A. J.; Hunter, C. A.; Sanders, J. K. M. Solvation and Surface Effects on Polymorph Stabilities at the Nanoscale. *Chem. Soc. Rev.* **2016**, *7*, 6617−6627.
(78) Warzecha, M.; Guo, R.; Bhardwaj, R. M.; Reutzel-Edens, S. M.; Price, S. L.; Lamprou, D. A.; Florence, A. J. Direct Observation of Templated Two-Step Nucleation Mechanism during Olanzapine Hydrate Formation. *Cryst. Growth Des.* **2017**, *17*, 6382−6393.
(79) Ngo, D.-T.; Kuhn, L. T. In Situ Transmission Electron Microscopy for Magnetic Nanostructures. *Adv. Nat. Sci. Nanosci. Nanotechnol.* **2016**, *7*, No. 045001.

https://doi.org/10.1021/acs.cgd.1c00723
Cryst. Growth Des. 2021, 21, 6254−6265